Compressive Detection of Random Subspace Signals

Alireza Razavi, Mikko Valkama, Danijela Cabric

arXiv:1507.02999v1 [cs.IT] 10 Jul 2015

Abstract

The problem of compressive detection of random subspace signals is studied. We consider signals modeled as $\mathbf{y} = \mathbf{H}\mathbf{x}$ where $\mathbf{H}$ is an $N \times K$ matrix with $K \leq N$ and $\mathbf{x} \sim \mathcal{N}(0, \sigma_x^2 \mathbf{I}_K)$. We say that signal $\mathbf{y}$ lies in or leans toward a subspace if the condition number of $\mathbf{H}\mathbf{H}^T$ is strictly greater than one. We first design a measurement matrix $\mathbf{\Phi} = [\mathbf{\Phi}_s^T, \mathbf{\Phi}_o^T]^T$ comprising of two sub-matrices $\mathbf{\Phi}_s$ and $\mathbf{\Phi}_o$ where $\mathbf{\Phi}_s$ projects the signals to the strongest left-singular vectors, i.e., the left-singular vectors corresponding to the largest singular values, of subspace matrix $\mathbf{H}$ and $\mathbf{\Phi}_o$ projects it to the weakest left-singular vectors. We then propose two detectors which work based on the difference in energies of the samples measured by two sub-matrices $\mathbf{\Phi}_s$ and $\mathbf{\Phi}_o$. Simplified versions of the proposed detectors for the case when the variance of noise is known are also provided. Furthermore, we study the performance of the detector when measurements are imprecise and show how imprecision can be compensated by employing more measurement devices. The problem is then re-formulated for the case when the signal lies in the union of a finite number of linear subspaces instead of a single linear subspace. Finally, we study the performance of the proposed methods by simulation examples.

Keywords

Compressive Detection, Random Subspace Signals, Hypothesis Testing, Unknown Noise Variance, Precision Budget, F-distribution

I. Introduction

The topic of sub-Nyquist sampling and Compressive Sensing (CS), where the effort is to draw inferences about the signal based on samples taken in rates lower than what suggested by Shannon-

A. Razavi and M. Valkama are with the Department of Electronics and Communications Engineering, Tampere University of Technology (TUT), Tampere, Finland. emails: alireza.razavi@tut.fi, mikko.e.valkama@tut.fi

D. Cabric is with Cognitive Reconfigurable Embedded Systems Lab (CORES), University of California Los Angeles (UCLA), CA. email:danijela@ee.ucla.edu

Nyquist sampling theorem, has been one of the most attractive topics in the area of signal processing for more than a decade. Compressive Sensing states that if a signal is sparse in some known bases, then it is possible to reconstruct it from a relatively few linear projections [1]–[3]. While most of the efforts in the area of CS has been devoted to the problem of estimation of a sparse signal from possibly noisy compressive measurements, there have been also efforts in accomplishing other signal processing task such as Compressive Detection [4]–[10], Compressive Classification [4], [11]–[14], etc. The goal of this paper is to study the problem of detecting a subspace signal from its sub-Nyquist measurements.

Signal detection [15] is an important task in Statistical Signal Processing where the goal is to decide on the presence/absence of a signal rather than estimating it. Signal Detection has applications in many areas of engineering and science, including wireless communications, radar and sonar, bioinformatics, etc. The literature on detection from Nyquist samples is very vast and well-studied; see, e.g., [15]–[17] and references therein. With the advent of sub-Nyquist sampling topic, like many other fields, there have also been additional efforts to tailor the existing signal detection techniques to the case where samples are taken in sub-Nyquist rates. The first criterion that a signal has to meet to qualify for being detectable based on sub-Nyquist samples is to be *sparse* in some known basis, or in a broader sense to lie in a *low-dimensional subspace* in the high-dimensional ambient space.

In this paper we address the problem of compressive detection of signals that lie on or close to a low dimensional linear subspace. We start with the simplest case when the signal is drawn from a known low-dimensional subspace and propose two tests for detection of signal from (down to) only two measurements. The main advantage of the proposed algorithm over the existing methods is that it does not need the knowledge of the noise variance to work. However, we also provide the simplified versions of the proposed methods for the case when the noise variance is known. We then study the effect of imprecise measurements and show that the imprecision can be compensated by employing more measurement devices. Then the proposed method is re-formulated for the case when the signal is lying on the union of a finite number of known linear subspaces with each of subspaces having a certain probability of being the subspace on which the signal truly lies. In other words, in this case, instead of having the exact knowledge of the subspace, we know the set of all subspaces from which the signal may emerge together with the corresponding probabilities that the signal may lie on each of them. We will introduce the optimum sampling strategy in this case and show that although the performance falls by increasing the number of possible subspaces, it remains reasonable as long as the cardinality of the set is much smaller than the ambient dimension.

Related work: In [4], [5] authors studied the problem of compressive detection, but they formulated

the problem for deterministic agnostic signals rather than random subspace signals. Besides, their methods did not take into consideration the unknown noise variance scenario. The method in [6] designs a matched subspace detector for subspace signals. The method assumes that the exact knowledge of signal is available for detector design. They extend their work to unknown signals in [7] but like the previous ones they need the variance of noise to design the compressive detector. The work of [9] provided upper bounds for probabilities of false alarm and mis-detection for deterministic signals while the variance of noise is known. Finally, in [10] authors studied the problem of compressive detection of random subspace signals but similar to the previously mentioned works the noise variance was assumed known.

Notations and Mathematical Preliminaries: Throughout this paper matrices and vectors are denoted by capital and small boldface letters, respectively. $=$ denotes the equality and $\triangleq$ denotes the definition. $\mathbb{E}_X$ is reserved for statistical expectation operator with respect to the random variable X, and $\otimes$ denotes the Kronecker product. $\mathbf{I}_P$, $\mathbf{1}_{P,Q}$ and $\mathbf{0}_{P,Q}$ represent $P \times P$ identity matrix, and $P \times Q$ all-one and all-zero matrix, respectively. For an arbitrary $M \times N$ matrix $\mathbf{A}$, $[\mathbf{A}]_{i,j}$ denotes the (i,j)-th entry of the matrix. For a set $\mathcal{M}$, cardinality of the set is shown as $|\mathcal{M}|$. For a matrix $\mathbf{A}$ we show its i-th eigenvalue by $\lambda_i(\mathbf{A})$. We also use the notations $\lambda_{\max}(\mathbf{A})$ and $\lambda_{\min}(\mathbf{A})$ for denoting its maximum and minimum eigenvalues, respectively.

Paper Organization: The rest of this paper is organized as follows: first, in Section II we explain the basic model of a linear subspace signal and we introduce the sampling strategy that we choose for our compressive detector. Then based on the introduced sampling strategy, in Section III we introduce two compressive detectors for detection of the signal based on the sub-Nyquist samples. We also briefly study the simplification when the noise variance is known as well as the case of subspace interference. Next, in Section IV, we study the effect of imprecise measurements where , e.g. because of hardware design limitations, the measurement matrix may deviate from the ideal one introduced in Section III. In Section V, we extend our design to the case where instead of knowing the exact linear subspace on which signal lies, we have only more coarse knowledge about the signal location in the ambient space in the form of knowing all the possibilities for the true subspace together with their corresponding probabilities. The performances of the proposed methods are studied through simulation results in Section VI. Finally we conclude the paper in Section VII.

II. System Model

Consider an $N \times 1$ signal $\mathbf{y}[n], n = 1, \ldots, N_b$, formed as a linear combination of a random subspace signal $\mathbf{H}\mathbf{x}[n]$, where $\mathbf{x}[n] \sim \mathcal{N}(\mathbf{0}, \sigma_s^2 \mathbf{I}_K)$, and a stationary noise vector $\mathbf{w}[n] \sim \mathcal{N}(\mathbf{0}, \sigma_0^2 \mathbf{I}_N)$:

$$\mathbf{y}[n] = \mathbf{H}\mathbf{x}[n] + \mathbf{w}[n], \tag{1}$$

where $\mathbf{H}$ is an $N \times K$ deterministic matrix with $K \leq N$. We denote N nonnegative eigenvalues of $\mathbf{H}\mathbf{H}^T$ by $\rho_1^2 \geq \rho_2^2 \geq \ldots \geq \rho_K^2 > \rho_{K+1}^2 = \rho_{K+2}^2 = \ldots = \rho_N^2 = 0$ and we assume that

$$\frac{\rho_1^2}{\rho_N^2} > 1. \tag{2}$$

Inequality (2) implies that the energy of signal is not distributed uniformly over all dimensions, or in other words, the signal lies in (or at least leans toward) some subspace of the ambient space.

Furthermore, we assume that $\mathbf{x}[n] \sim \mathcal{N}(\mathbf{0}_{K,1}, \sigma_x^2 \mathbf{I}_K),\ n = 1, \ldots, N_b$. The goal of this paper is to study the problem of signal detection in (1) or, in other words, performing the following statistical test

$$\begin{cases} \mathcal{H}_0 : \mathbf{y}[n] = \mathbf{w}[n], \\ \mathcal{H}_1 : \mathbf{y}[n] = \mathbf{H}\mathbf{x}[n] + \mathbf{w}[n], \end{cases} \tag{3}$$

based on N_b compressive observations

$$\mathbf{z}[n] = \mathbf{\Phi}\mathbf{y}[n],\ n = 1, \ldots, N_b, \tag{4}$$

where $\mathbf{\Phi}$ is the $M \times N$ observation matrix with $M \ll N$. Parameter M denotes the number of measurement devices where each row of the measurement matrix $\mathbf{\Phi}$ in fact represents a measurement device.

This problem was addressed in [6], [7] in presence of noise with known variance. Here we design the sub-Nyquist detectors without assuming prior noise knowledge. To this end, we partition the M measurement devices to two sets or, in other words, we consider the measurement matrix $\mathbf{\Phi}$ in (4) to consist of two sub-matrices: the $M_1 \times N$ matrix $\mathbf{\Phi}_s$ and the $M_2 \times N$ matrix $\mathbf{\Phi}_o$ as

$$\mathbf{\Phi} = \begin{bmatrix} \mathbf{\Phi}_s \\ \mathbf{\Phi}_o \end{bmatrix}, \tag{5}$$

While the rows of $\mathbf{\Phi}_s$ lie in the M_1-dimensional subspace spanned by the M_1 strongest (in terms of magnitude of the corresponding singular values) left singular vectors of $\mathbf{H}$, the M_2 rows of sub-matrix $\mathbf{\Phi}_o$ lie in the M_2-dimensional subspace spanned by the M_2 weakest left singular vectors of $\mathbf{H}$. We demonstrate the corresponding outputs of these two sets of measurement devices by $\mathbf{z}_s = \mathbf{\Phi}_s\mathbf{y}$ and $\mathbf{z}_o = \mathbf{\Phi}_o\mathbf{y}$, respectively. When the signal exist, i.e. $\mathbf{x} \neq \mathbf{0}$, the above design results in big difference

between the variance of the measurements $\mathbf{z}_s$ and $\mathbf{z}_o$. On the other hand, when the signal does not exist, $\mathbf{z}_s$ and $\mathbf{z}_o$ have similar variances. This difference in the variance of the outputs of the two sub matrices is what we will exploit to design compressive detectors in the next section.

III. Compressive Subspace Detection

Based on the system model of the previous section, in this section we propose two detectors for performing the hypothesis testing problem of (3). Both detectors are composed of two sets of measurement devices, represented by $\mathbf{\Phi}_s$ and $\mathbf{\Phi}_o$. In the sequel we introduce these two detectors and derive their performance measures. The performance of the two proposed detectors will be studied in Section VI through simulation experiments.

A. Maximally-Uncorrelated Compressive Detector

Assume that the SVD of matrix $\mathbf{H}$ is given by

$$\mathbf{H} = \mathbf{U}\mathbf{D}\mathbf{V}^T. \tag{6}$$

Consider positive integers M_1 and M_2 such that $M = M_1 + M_2$. Let us denote the first M_1 columns of $\mathbf{U}$ by $\mathbf{U}_s$ and its last M_2 by $\mathbf{U}_o$. We propose the following design for $M \times N$ measurement matrix $\mathbf{\Phi} = \begin{bmatrix} \mathbf{\Phi}_s \\ \mathbf{\Phi}_o \end{bmatrix}$ with sub-matrices $\mathbf{\Phi}_s$ and $\mathbf{\Phi}_o$ defined as

$$\mathbf{\Phi}_s \triangleq \frac{1}{\sqrt{M}}\mathbf{T}_s\mathbf{U}_s^T, \tag{7}$$

and

$$\mathbf{\Phi}_o \triangleq \frac{1}{\sqrt{M}}\mathbf{T}_o\mathbf{U}_o^T, \tag{8}$$

where $\mathbf{T}_s$ and $\mathbf{T}_o$ are $M_1 \times M_1$ and $M_2 \times M_2$ unitary matrices, respectively. The term $\frac{1}{\sqrt{M}}$ in (7) and (8) is to guarantee that the received energy at the output of the sub-Nyquist sampler is independent of the number of samplers. This makes the study of the effect of the number of samplers on the performance fair as otherwise it is obvious that the bigger is the number of samplers the better is the performance. We remark that M rows of the measurement matrix $\mathbf{\Phi}$ represent M measurement devices equipped to collect samples. Hereafter, we use the terms *measurement matrix* and *measurement devices* interchangeably.

The reason for choosing this design for measurement matrix is that the rows of $\mathbf{\Phi}_s$ span the M_1-dimensional subspace which contains the highest amount of energy of signal $\mathbf{Hx}$, or in other words, is the M_1-dimensional subspace along which the variance of $\mathbf{Hx}$ is maximized. Furthermore, the rows of $\mathbf{\Phi}_o$

span the M_2-dimensional subspace which contains the lowest amount of energy of signal $\mathbf{Hx}$, or in other words, is the M_2-dimensional subspace along which the variance of $\mathbf{Hx}$ is minimized. The difference between the energy of signal taken at the output of these two sub-matrices can then be exploited for detection of signal. The following theorem, justifies the above discussion.

Theorem 1. *The measurement sub-matrix $\mathbf{\Phi}_s$ in (7) is the solution to the following optimization problem*

$$\arg\max_{\mathbf{\Phi}_s} \mathbb{E}_{\mathbf{x},\mathbf{w}}(\|\mathbf{z}_s\|_2^2), \quad \text{s.t.} \quad M\mathbf{\Phi}_s\mathbf{\Phi}_s^T = \mathbf{I}_{M_1}, \tag{9}$$

In other words, the rows of $\mathbf{\Phi}_s$ in (7) represent the set of M_1 uncorrelated measurement devices that maximize the expected value of total energy (or the total variance) in their outputs.

Correspondingly, the measurement sub-matrix $\mathbf{\Phi}_o$ in (8) is the solution to the following optimization problem

$$\arg\min_{\mathbf{\Phi}_o} \mathbb{E}_{\mathbf{x},\mathbf{w}}(\|\mathbf{z}_o\|_2^2), \quad \text{s.t.} \quad M\mathbf{\Phi}_o\mathbf{\Phi}_o^T = \mathbf{I}_{M_2}, \tag{10}$$

In other words, the rows of $\mathbf{\Phi}_o$ in (8) represent the set of M_2 uncorrelated measurement devices that minimize the expected value of total energy (or the total variance) in their outputs.

Proof: We first notice that

$$\begin{aligned} \mathbb{E}_{\mathbf{x},\mathbf{w}}(\|\mathbf{z}_s\|_2^2) &= \mathbb{E}_{\mathbf{x}}(\mathbf{x}^T\mathbf{H}^T\mathbf{\Phi}_s^T\mathbf{\Phi}\mathbf{H}\mathbf{x}) + \frac{M_1\sigma_0^2}{M} \\ &= \sigma_x^2 \text{trace}(\mathbf{H}\mathbf{H}^T\mathbf{\Phi}_s^T\mathbf{\Phi}_s) + \frac{M_1\sigma_0^2}{M} \end{aligned} \tag{11}$$

Noticing that the second term in the right-hand side of (11) is independent of measurement design and $\mathbf{H}^T\mathbf{H}$ and $\mathbf{\Phi}_s^T\mathbf{\Phi}_s$ are both symmetric matrices and that $M_1\mathbf{\Phi}_s^T\mathbf{\Phi}_s$ in (9) has M_1 eigenvalues equal to 1 and $N - M_1$ eigenvalues equal to zero, the proof of (7) is easily concluded by employing von Neumann trace theorem [18, P 11.4.5], [19, Theorem 6.77]. The proof for (8) is similar. ■

We call the measurement design in (7) and (8) *Maximally-Uncorrelated compressive detector* as it is the optimum design when the measurements are uncorrelated.

Next, based on the above measurement design we introduce a test statistic for carrying out the hypothesis testing problem of (3). The following theorem states this test and derives its performance measures.

Theorem 2. *Consider the following test for performing the hypothesis testing problem given in (3) based*

on compressive measurements $\mathbf{z}[n] = \mathbf{\Phi}\mathbf{y}[n],\ n = 1, \ldots, N_b$

$$\mathcal{T} = \frac{\sum_{n=1}^{N_b} \mathbf{z}_s[n]^T \mathbf{z}_s[n]}{\sum_{n=1}^{N_b} \mathbf{z}_o[n]^T \mathbf{z}_o[n]} \underset{\mathcal{H}_0}{\overset{\mathcal{H}_1}{\gtrless}} \gamma. \tag{12}$$

The Probability of False Alarm, P_{FA}*, for this test is computed as*

$$P_{FA} = \mathbb{Q}_{F(M_1 N_b, M_2 N_b)}(\gamma), \tag{13}$$

and the Probability of Detection, P_D*, is bounded as*

$$P_{D,lb} \leq P_D \leq P_{D,ub} \tag{14}$$

where $P_{D,lb}$ *and* $P_{D,ub}$ *are, respectively, the lower bound and the upper bound for the probability of detection which will take the following formulas*

$$P_{D,lb} = \mathbb{Q}_{F(M_1 N_b, M_2 N_b)}(\eta_{lb}\gamma), \tag{15}$$

and

$$P_{D,ub} = \mathbb{Q}_{F(M_1 N_b, M_2 N_b)}(\eta_{ub}\gamma), \tag{16}$$

where $\eta_{lb} \triangleq \frac{\sigma_0^2 + \sigma_x^2 \rho_{N-M_2+1}^2}{\sigma_0^2 + \sigma_x^2 \rho_{M_1}^2}$*,* $\eta_{ub} \triangleq \frac{\sigma_0^2 + \sigma_x^2 \rho_N^2}{\sigma_0^2 + \sigma_x^2 \rho_1^2}$*, and* $\mathbb{Q}_{F(d_1,d_2)}(x)$ *is the tail probability of the* F*-distribution with parameters (degrees of freedom)* d_1 *and* d_2 *at point* x*.*

Proof: To prove the theorem, we first notice that $\mathbf{z}_o[n]$ has distribution

$$\mathbf{z}_o[n] \sim \begin{cases} \mathcal{N}(\mathbf{0}, \frac{\sigma_0^2}{M}\mathbf{I}_{M_1}) & \text{under } \mathcal{H}_0, \\ \\ \mathcal{N}(\mathbf{0}, \frac{1}{M}(\sigma_0^2 \mathbf{I}_{M_2} + \sigma_x^2 \mathbf{T}_o \mathbf{\Lambda}_o \mathbf{T}_o^T)) & \text{under } \mathcal{H}_1, \end{cases} \tag{17}$$

where $\mathbf{\Lambda}_o$ is an $M_2 \times M_2$ diagonal matrix whose (i,i)-th diagonal element is $\rho_{N-M_2+i}^2$.

On the other hand, the distribution of $\mathbf{z}_s$ is

$$\mathbf{z}_s[n] \sim \begin{cases} \mathcal{N}(\mathbf{0}, \frac{\sigma_0^2}{M}\mathbf{I}_{M_1}) & \text{under } \mathcal{H}_0, \\ \\ \mathcal{N}(\mathbf{0}, \frac{1}{M}(\sigma_0^2 \mathbf{I}_{M_1} + \sigma_x^2 \mathbf{T}_s \mathbf{\Lambda}_s \mathbf{T}_s^T)) & \text{under } \mathcal{H}_1, \end{cases} \tag{18}$$

where $\mathbf{\Lambda}_s$ is an $M_1 \times M_1$ diagonal matrix whose (i,i)-th diagonal element is ρ_i^2.

From (18) we have

$$\frac{\sum_{n=1}^{N_b} \mathbf{z}_s[n]^T \mathbf{z}_s[n]}{\sigma_0^2/M} \sim \mathcal{X}_{M_1 N_b}^2, \text{under } \mathcal{H}_0, \tag{19}$$

where $\mathcal{X}_d^2$ denotes chi-squared distribution with d degrees of freedom [15]. On the other hand, under $\mathcal{H}_1$ we have

$$\sum_{n=1}^{N_b} \mathbf{z}_s[n]^T \mathbf{A}_s^{-1} \mathbf{z}_s[n] \sim \mathcal{X}^2_{M_1 N_b}, \text{under } \mathcal{H}_1. \tag{20}$$

where $\mathbf{A}_s \triangleq \frac{1}{M}(\sigma_0^2 \mathbf{I}_{M_1} + \sigma_x^2 \mathbf{T}_s \mathbf{\Lambda}_s \mathbf{T}_s^T)$. From Rayleigh-Ritz theorem [20, Chapter 8] we know that

$$\lambda_{\min}(\mathbf{A}_s^{-1}) \mathbf{z}_s^T \mathbf{z}_s \leq \mathbf{z}_s^T \mathbf{A}_s^{-1} \mathbf{z}_s \leq \lambda_{\max}(\mathbf{A}_s^{-1}) \mathbf{z}_s^T \mathbf{z}_s \tag{21}$$

where $\lambda_{\min}(\mathbf{A}_s^{-1}) = \frac{1}{\lambda_{\max}(\mathbf{A}_s)} = \frac{M}{\sigma_0^2 + \sigma_x^2 \rho_1^2}$ and $\lambda_{\max}(\mathbf{A}_s^{-1}) = \frac{1}{\lambda_{\min}(\mathbf{A}_s)} = \frac{M}{\sigma_0^2 + \sigma_x^2 \rho_{M_1}^2}$.

Similarly, from (17) we have

$$\frac{\sum_{n=1}^{N_b} \mathbf{z}_o[n]^T \mathbf{z}_o[n]}{\sigma_0^2 / M} \sim \mathcal{X}^2_{M_1 N_b}, \text{under } \mathcal{H}_0, \tag{22}$$

and

$$\sum_{n=1}^{N_b} \mathbf{z}_o[n]^T \mathbf{A}_o^{-1} \mathbf{z}_o[n] \sim \mathcal{X}^2_{M_2 N_b}, \text{under } \mathcal{H}_1. \tag{23}$$

where $\mathbf{A}_o \triangleq \frac{1}{M}(\sigma_0^2 \mathbf{I}_{M_2} + \sigma_x^2 \mathbf{T}_o \mathbf{\Lambda}_o \mathbf{T}_o^T)$. We also have

$$\lambda_{\min}(\mathbf{A}_o^{-1}) \mathbf{z}_o^T \mathbf{z}_o \leq \mathbf{z}_o^T \mathbf{A}_o^{-1} \mathbf{z}_o \leq \lambda_{\max}(\mathbf{A}_o^{-1}) \mathbf{z}_s^T \mathbf{z}_s \tag{24}$$

where $\lambda_{\min}(\mathbf{A}_o^{-1}) = \frac{1}{\lambda_{\max}(\mathbf{A}_o)} = \frac{M}{\sigma_0^2 + \sigma_x^2 \rho_{N-M_2+1}^2}$ and $\lambda_{\max}(\mathbf{A}_o^{-1}) = \frac{1}{\lambda_{\min}(\mathbf{A}_o)} = \frac{M}{\sigma_0^2 + \sigma_x^2 \rho_N^2}$.

From above computations, under $\mathcal{H}_0$ hypothesis we will have

$$\frac{\sum_{n=1}^{N_b} \mathbf{z}_s[n]^T \mathbf{z}_s[n]}{\sum_{n=1}^{N_b} \mathbf{z}_o[n]^T \mathbf{z}_o[n]} \sim F_{M_1 N_b, M_2 N_b}, \text{under } \mathcal{H}_0. \tag{25}$$

Under $\mathcal{H}_1$ hypothesis we have

$$\frac{\frac{\sum_{n=1}^{N_b} \mathbf{z}_s[n]^T \mathbf{z}_s[n]}{(\sigma_0^2 + \sigma_x^2 \rho_1^2)/M}}{\frac{\sum_{n=1}^{N_b} \mathbf{z}_o[n]^T \mathbf{z}_o[n]}{(\sigma_0^2 + \sigma_x^2 \rho_N^2)/M}} \leq \frac{\sum_{n=1}^{N_b} \mathbf{z}_s[n]^T \mathbf{A}_s^{-1} \mathbf{z}_s[n]}{\sum_{n=1}^{N_b} \mathbf{z}_o[n]^T \mathbf{A}_o^{-1} \mathbf{z}_o[n]} \sim F_{M_1 N_b, M_2 N_b} \tag{26}$$

and similarly

$$\frac{\frac{\sum_{n=1}^{N_b} \mathbf{z}_s[n]^T \mathbf{z}_s[n]}{(\sigma_0^2 + \sigma_x^2 \rho_{M_1}^2)/M}}{\frac{\sum_{n=1}^{N_b} \mathbf{z}_o[n]^T \mathbf{z}_o[n]}{(\sigma_0^2 + \sigma_x^2 \rho_{N-M_2+1}^2)/M}} \geq \frac{\sum_{n=1}^{N_b} \mathbf{z}_s[n]^T \mathbf{A}_s^{-1} \mathbf{z}_s[n]}{\sum_{n=1}^{N_b} \mathbf{z}_o[n]^T \mathbf{A}_o^{-1} \mathbf{z}_o[n]} \sim F_{M_1 N_b, M_2 N_b} \tag{27}$$

From (25), (26), and (27) the proof is concluded. ■

Remark 1: The $\mathbb{Q}$-function of F-distribution is expressed as [21]

$$\mathbb{Q}_{F(d_1,d_2)}(x) = 1 - I_{\frac{d_1 x}{d_1 x + d_2}}(\frac{d_1}{2}, \frac{d_2}{2}), \tag{28}$$

where $I_x(a,b)$ is the *regularized incomplete Beta function* defined as

$$I_x(a,b) = \frac{B(x;a,b)}{B(a,b)}, \tag{29}$$

where $B(x;a,b) \triangleq \int_0^x t^{a-1}(1-t)^{b-1}dt$ is the *incomplete Beta function* and $B(a,b) \triangleq B(1;a,b)$ is the *Beta function*. □

Remark 2: From Theorem 2 it is clear that for a given M_1 and M_2 the proposed detector is *unbiased* [17, Chapter 4] if $\rho_{N-M_2+1} < \rho_{M_1}$. Furthermore, if the condition number $\mathrm{cond}(\mathbf{H}\mathbf{H}^T) \triangleq \frac{\rho_1^2}{\rho_N^2} > 1$, then there is a design as suggested in this section with certain M_1 and M_2 which delivers an unbiased detector. □

Remark 3: While Theorem 2 proposes a test statistic for signal detection and provides a proof for the performance of the proposed detector, it does not provide us with the optimum number of samplers M_1 and M_2. We will study the impact of M_1 and M_2 on the performance of the proposed detector in Section VI via simulation examples. From a practical point of view an important factor which may limit utilizing high values of M_1 and M_2 is the hardware cost and complexity as it is proportional to the number of samplers which is in turn determined by M_1 and M_2. □

B. Fully-Correlated Compressive Detector

In this part, we study the effect of increasing the Signal-to-Noise Ratio (SNR) at the expense of uncorrelatedness of measurement devices. For a certain measurement device, the effective noise energy can be decreased (and therefore the SNR can be increased) by repeating the measurements and averaging over all of them. Collecting the multiple measurements one after the other over time for enhancing the effective SNR is not however a suitable solution here, firstly because the signal itself is random too, and secondly because it increases the *latency* which is an issue in many applications such as radar or wireless communications due to the relatively quick changes of communication channel characteristics.

However in our proposed measurement framework, improving the effective SNR can be done by employing M_1 identical measurement vectors instead of $M_1 \times N$ measurement matrix $\mathbf{\Phi}_s$ in (7) and M_2 identical measurement vectors instead of $M_2 \times N$ measurement matrix $\mathbf{\Phi}_o$ in (8) and then averaging over all measurements. This will not increase the latency because the identical measurements are taken in parallel. In other words, matrices $\mathbf{\Phi}_s$ and $\mathbf{\Phi}_o$ in (7) and (8) should be respectively redefined as

$$\mathbf{\Phi}_s \triangleq \frac{1}{\sqrt{M}} \mathbf{1}_{M_1,1} \otimes \mathbf{u}_1^T, \tag{30}$$

and

$$\mathbf{\Phi}_o \triangleq \frac{1}{\sqrt{M}}\mathbf{1}_{M_2,1} \otimes \mathbf{u}_N^T, \tag{31}$$

where $\mathbf{u}_1$ and $\mathbf{u}_N$ are the left singular vectors of $\mathbf{H}$ corresponding to the ρ_1 and ρ_N, respectively. The following theorem is to show the significance of the measurement design in (30) and (31).

Theorem 3. *The measurement sub-matrix $\mathbf{\Phi}_s$ in (30) is the solution to the following optimization problem*

$$\arg\max_{\mathbf{\Phi}} \mathbb{E}_{\mathbf{x},\mathbf{w}}(\|\mathbf{z}_s\|_2^2). \tag{32}$$

In other words, the rows of $\mathbf{\Phi}_s$ in (30) represent the set of M_1 measurement devices that maximize the total energy (or the total variance) in their outputs.

Correspondingly, the measurement sub-matrix $\mathbf{\Phi}_o$ in (31) is the solution to the following optimization problem

$$\arg\min_{\mathbf{\Phi}} \mathbb{E}_{\mathbf{x},\mathbf{w}}(\|\mathbf{z}_s\|_2^2). \tag{33}$$

In other words, the rows of $\mathbf{\Phi}_o$ in (31) represent the set of M_2 measurement devices that minimize the total energy (or the total variance) in their outputs.

Proof: We first notice that

$$\begin{aligned}\mathbb{E}_{\mathbf{x},\mathbf{w}}(\|\mathbf{z}_s\|_2^2) &= \mathbb{E}_{\mathbf{x}}(\mathbf{x}^T\mathbf{H}^T\mathbf{\Phi}_s^T\mathbf{\Phi}\mathbf{H}\mathbf{x}) + \frac{M_1\sigma_0^2}{M} \\ &= \sigma_x^2 \mathrm{trace}(\mathbf{H}\mathbf{H}^T\mathbf{\Phi}_s^T\mathbf{\Phi}_s) + \frac{M_1\sigma_0^2}{M}\end{aligned} \tag{34}$$

Since the second term on the right-hand side of (34) is independent of measurement design, the optimum design for $\mathbf{\Phi}_s$ is the one which maximizes the first term. Noticing that $\mathbf{H}^T\mathbf{H}$ and $\mathbf{\Phi}_s^T\mathbf{\Phi}_s$ are both symmetric, from [18, P 11.4.5] we have

$$\mathrm{trace}(\mathbf{H}\mathbf{H}^T\mathbf{\Phi}_s\mathbf{\Phi}_s^T) \leq \sum_{i=1}^{M_1} \rho_i^2 \lambda_i(\mathbf{\Phi}_s\mathbf{\Phi}_s^T) \tag{35}$$

Unlike Theorem 1, here we have no constraint on matrix $\mathbf{\Phi}_s$ other than its rows have norm $1/\sqrt{M}$ which means that $\mathrm{trace}(\mathbf{\Phi}_s\mathbf{\Phi}_s^T) = \sum_{i=1}^{M_1} \lambda_i(\mathbf{\Phi}_s\mathbf{\Phi}_s^T) = M_1/M$. Therefore the design of $\mathbf{\Phi}_s$ can be done in two steps. In the first step we find the eigenvalues $\{\lambda_i(\mathbf{\Phi}_s\mathbf{\Phi}_s^T)\}_{i=1}^{M_1}$ that maximize the right-hand side of inequality (34). From [22, 4.B.7 and 1.A] the maximum is attained when $\lambda_1(\mathbf{\Phi}_s\mathbf{\Phi}_s^T)\} = 1$ and $\{\lambda_i(\mathbf{\Phi}_s\mathbf{\Phi}_s^T)\}_{i=2}^{M_1} = 0$. In the second step we simply employ [18, P 11.4.5] to conclude the proof of (30) being the solution to (32). The proof for (31) is similar. ■

After designing the samplers as in (30) and (31) and collecting measurement vectors $\mathbf{z}_s[n]$ and $\mathbf{z}_o[n]$, the effective energy of noise can then be reduced by averaging over all elements of $\mathbf{z}_s[n]$ and $\mathbf{z}_o[n]$ to obtain

$$\bar{z}_s[n] = \frac{1}{M_1}\mathbf{1}_{1,M_1}\mathbf{z}_s[n],\ \ n = 1, \ldots, N_b, \tag{36}$$

and

$$\bar{z}_o[n] = \frac{1}{M_2}\mathbf{1}_{1,M_2}\mathbf{z}_o[n],\ \ n = 1, \ldots, N_b. \tag{37}$$

In other words, instead of choosing M_1 rows of $\mathbf{\Phi}_s$ that span the M_1-dimensional subspace along which the energy of signal is maximum as in Section III-A, we choose M_1 identical rows for $\mathbf{\Phi}_s$ each as the 1-dimensional subspace along which the energy of signal is maximum, and then decrease the noise power (and therefore increase the effective SNR) by averaging over all M_1 measurements. Similarly, for $\mathbf{\Phi}_o$, instead of choosing its M_2 rows that span the M_2-dimensional subspace along which the energy of signal is minimum as in Section III-A, we choose M_2 identical rows for $\mathbf{\Phi}_o$ each as the 1-dimensional subspace along which the energy of signal is minimum, and thus decrease the noise energy (and therefore increase the effective SNR) by averaging over all M_2 measurements.

The following theorem introduces the test for performing (3) based on measurement design in (30) and (31).

Theorem 4. *Consider the following test for compressive detection of subspace signal* $\mathbf{Hx}$

$$\mathcal{T} = \frac{M_1 \sum\limits_{n=1}^{N_b} |\bar{z}_s[n]|^2}{M_2 \sum\limits_{n=1}^{N_b} |\bar{z}_o[n]|^2} \underset{\mathcal{H}_0}{\overset{\mathcal{H}_1}{\gtrless}} \gamma \tag{38}$$

The probability of false alarm P_{FA} *and the probability of detection* P_D *are then expressed as*

$$P_{FA} = \mathbb{Q}_{F(N_b,N_b)}(\gamma), \tag{39}$$

and

$$P_D = \mathbb{Q}_{F(N_b,N_b)}\Big(\frac{\sigma_0^2 + M_2\sigma_x^2\rho_N^2}{\sigma_0^2 + M_1\sigma_x^2\rho_1^2}\gamma\Big). \tag{40}$$

Proof: To derive the probability of false alarm P_{FA} and the probability of detection P_{D}, we first notice that if the Gaussian noise is i.i.d, then it is easy to observe that the distribution of $\bar{z}_o[n]$ is

$$\bar{z}_o[n] \sim \begin{cases} \mathcal{N}(0, \frac{\sigma_0^2}{MM_2}) & \text{under } \mathcal{H}_0, \\ \\ \mathcal{N}(0, \frac{\sigma_0^2}{MM_2} + \frac{1}{M}\sigma_x^2\rho_N^2) & \text{under } \mathcal{H}_1. \end{cases} \tag{41}$$

Similarly, the distribution of $\bar{z}_s[n]$ is

$$\bar{z}_s[n] \sim \begin{cases} \mathcal{N}(0, \frac{\sigma_0^2}{MM_1}) & \text{under } \mathcal{H}_0, \\ \\ \mathcal{N}(0, \frac{\sigma_0^2}{MM_1} + \frac{1}{M}\sigma_x^2\rho_1^2) & \text{under } \mathcal{H}_1, \end{cases} \tag{42}$$

Then by following steps similar to those in Theorem 2, (39) and (40) are concluded. ■

Opposite to the Maximally Uncorrelated Detector introduced in Section III-A, the performance of Fully Correlated Detector has a clear connection to the way we choose the number of samplers. The following Corollary discusses this.

Corollary III.1. *For a given number of samplers M and probability of false alarm P_{FA}, the performance of the detector P_D is maximized when $M_2 = 1$ and $M_1 = M - 1$.*

Proof: First, we notice from (39) that the threshold level γ is independent of the choice of M_1 and M_2. Then from (40) it is clear that P_{D} achieves its maximum value when M_2 reaches its minimum value and M_1 reaches its maximum value. ■

The above Corollary asserts that in the case of Fully-Correlated Detector, for a fixed hardware budget, in terms of the total number of samplers $M = M_1 + M_2$, the best performance, in terms of P_{D}, is obtained if we employ just one sampler for $\mathbf{\Phi}_o$ and spend the rest of the hardware budget on $\mathbf{\Phi}_s$.

As we mentioned in Section III-A, the performance of Maximally-Uncorrelated Detector, however, does not exhibit such a straightforward relation to the number of samplers. Figure 1 demonstrates how the probability of detection for these two detectors changes with the number of maximum energy samplers M_1. As it can be observed, while the performance of Fully-Correlated Detector clearly enhances with increasing M_1, the performance of Maximally-Uncorrelated Detector does not show such a monotonic relationship.

Remark 4: Comparing (32) and (33) to (9) and (10) it may seem that the performance of the Fully-Correlated detector is always superior to the Maximally-Uncorrelated Detector as the optimizations in (32) and (33) are unconstrained compared to the optimizations in (9) and (10) which are constrained. However, we should notice that this is not always the case as Maximally-Uncorrelated Detector provides a higher *diversity* in its collected samples, which is reflected by the higher degrees of freedom in (13), (15) and (16) compared to (39) and (40). For example consider the case when $\mathbf{s}[n]$ is present but lies orthogonal to the strongest right singular vector of $\mathbf{H}$. Then for the Fully-Correlated samplers the energy of samples collected by all of the M_1 samplers $\mathbf{\Phi}_s$ includes only the energy of noise while for the

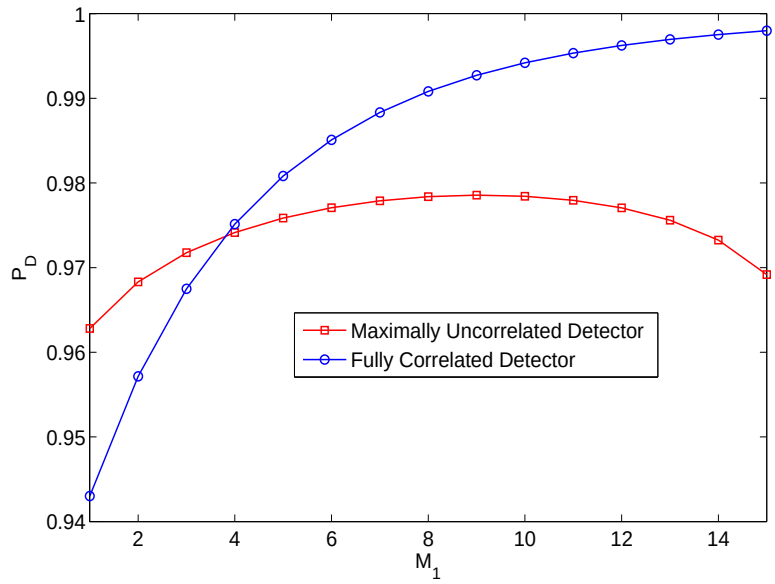

Fig. 1. Probability of Detection as a function of M_1 for the two detectors introduced in Sections III-A and III-B. The total number of samplers is $M = 16$, the Signal-to-Noise Ratio is $\frac{\sigma_x^2}{\sigma_0^2} = -20\text{dB}$ and the largest and smallest eigenvalues of $\mathbf{H}\mathbf{H}^T$ are $\rho_1^2 = 10$ and ρ_N^2=1, respectively.

Maximally-Uncorrelated Detector only the output energy of the first sampler is equivalent to the noise energy and the output of the rest of $M_1 - 1$ samplers include both the signal and the noise energy. □

C. Special Case of Known Noise Variance

As discussed earlier in this Section, the idea of having two sets of measurement devices $\mathbf{\Phi}_s$ and $\mathbf{\Phi}_o$ is to have two sets of measurements with maximum difference in their variances when the signal truly exists and equivalent variances when the signal does not exist and then making decision about the existence of signal based on this difference. However, if the variance of noise is known, we can simplify the proposed design by discarding $\mathbf{\Phi}_o$ as we can simply compare the variance of the output of $\mathbf{\Phi}_s$ to the known noise variance. In other words, we can employ only M_1 measurement devices determined by the rows of $\mathbf{\Phi}_s$ and then compare the power of measurements taken by them to the power of noise: if they are almost the same then we decide that no signal exists, if not then we decide that signal exists.

Similar to the two detectors proposed in sections III-A and III-B, we can have two detectors when the noise variance is known. The following two propositions express these two detectors and their

performances. We remark that since $\mathbf{\Phi}_o$ is discarded when noise variance is known, we will have $M_2 = 0$ and therefore the whole number of measurement devices is $M = M_1$.

Proposition III.1. *If we design the measurement matrix according to (7), then in the case of known σ_0^2, the test in (12) can be replaced by*

$$\mathcal{T} = \frac{\sum_{n=1}^{N_b} \mathbf{z}_s[n]^T \mathbf{z}_s[n]}{\sigma_0^2/M_1} \underset{\mathcal{H}_0}{\overset{\mathcal{H}_1}{\gtrless}} \gamma. \tag{43}$$

The Probability of False Alarm, P_{FA}, for this test is computed as

$$P_{FA} = \mathbb{Q}_{\chi^2(M_1 N_b)}(\gamma), \tag{44}$$

and the Probability of Detection, P_D, is bounded as

$$P_{D,lb} \leq P_D \leq P_{D,ub} \tag{45}$$

where $P_{D,lb}$ and $P_{D,ub}$ are, respectively, the lower bound and the upper bound for the probability of detection which will take the following formulas

$$P_{D,lb} = \mathbb{Q}_{\chi^2(M_1 N_b)}(\eta'_{lb}\gamma), \tag{46}$$

and

$$P_{D,ub} = \mathbb{Q}_{\chi^2(M_1 N_b)}(\eta'_{ub}\gamma), \tag{47}$$

where $\eta'_{lb} \triangleq \frac{\sigma_0^2}{\sigma_0^2+\sigma_x^2\rho_{M_1}^2}$, $\eta'_{ub} \triangleq \frac{\sigma_0^2}{\sigma_0^2+\sigma_x^2\rho_1^2}$, and $\mathbb{Q}_{\chi^2(d)}(x)$ is the tail probability of the chi-squared distribution with parameter (degree of freedom) d at point x.

Proposition III.2. *If we design the measurement matrix according to (30), then in the case of known σ_0^2, the test in (38) can be replaced by*

$$\mathcal{T} = \frac{\sum_{n=1}^{N_b} |\bar{z}_s[n]|^2}{\sigma_0^2/M_1^2} \underset{\mathcal{H}_0}{\overset{\mathcal{H}_1}{\gtrless}} \gamma \tag{48}$$

The Probability of False Alarm, P_{FA}, for this test is

$$P_{FA} = \mathbb{Q}_{\chi^2(N_b)}(\gamma), \tag{49}$$

and

$$P_D = \mathbb{Q}_{\chi^2(N_b)}\Big(\frac{\sigma_0^2}{\sigma_0^2 + M_1\sigma_x^2\rho_1^2}\gamma\Big). \tag{50}$$

D. Compressive Detection in Presence of Known Subspace Interference

Extending the above results to the subspace interference case is straightforward and is similar to the same scenario for detection of subspace signals in presence of interference [23]. Assume that the received signal model in (1) is replaced by

$$\mathbf{y}[n] = \mathbf{H}\mathbf{x}[n] + \mathbf{G}\mathbf{t}[n] + \mathbf{w}[n], \tag{51}$$

where $\mathbf{G}$ is an $N \times K'$ matrix. To solve the problem and formulate the detector, we can first cancel the interference term by projecting the measurement vector $\mathbf{y}[n]$ on the null subspace of interference signal, $\mathbf{P}_{\mathbf{G}}^{\perp} = \mathbf{G}(\mathbf{G}^T\mathbf{G})^{-1}\mathbf{G}^T$, and then design the measurement vectors as singular vectors of $\mathbf{P}_{\mathbf{G}}^{\perp}\mathbf{H}$ and apply the detection methods proposed in this section on the resulting interference-free measurements $\mathbf{P}_{\mathbf{G}}^{\perp}\mathbf{y}[n],\ n = 1, \ldots, N_b$.

IV. Compressive Detector with Non-Ideal Measurements

In this section we investigate the case when due to the lack of complete knowledge about the subspace or due to the limitations in designing hardware with infinite precision, the measurement vectors do not exactly match the singular vectors of matrix $\mathbf{H}$. We consider two models for describing this uncertainty. The first model, defines the finite precision using a measurement noise. The second model, on the other hand, chooses the measurement vector from a set of realizable measurement vectors (hardware) which are approximations (or quantized versions) of infinite-precision real-valued singular vectors.

A. Compressive Detection with Imprecise Measurements

In this section we analyze the detector when the measurement device is not precise. This imprecision in measurements can be modeled as [24]

$$\mathbf{z}[n] = \mathbf{\Phi}\mathbf{y}[n] + \delta^{-1/2}\boldsymbol{\epsilon}[n] \tag{52}$$

where $\boldsymbol{\epsilon}[n] \sim \mathcal{N}(0, 1)$ is the measurement noise and δ represents the precision of measurements.

If we select the same test statistic as in (12), then it can be easily verified that the probability of false alarm will be the same as in (13), but the lower and upper bounds of probability of detection in (15) and (16) will be replaced by

$$P_{D,lb} = \mathbb{Q}_{F(M_1N_b, M_2N_b)}\left(\frac{\sigma_0^2 + \sigma_x^2\rho_{N-M_2+1}^2 + M\delta^{-1}}{\sigma_0^2 + \sigma_x^2\rho_{M_1}^2 + M\delta^{-1}}\gamma\right), \tag{53}$$

and

$$P_{D,ub} = \mathbb{Q}_{F(M_1N_b, M_2N_b)}\left(\frac{\sigma_0^2 + \sigma_x^2\rho_{N}^2 + M\delta^{-1}}{\sigma_0^2 + \sigma_x^2\rho_{1}^2 + M\delta^{-1}}\gamma\right), \tag{54}$$

respectively. Comparing (53) and (54) with (15) and (16), it is clear that the performance degrades as the precision of measurement devices δ decreases. This can be however compensated by improving the precision through employing several, say L, identical measurement devices instead of each device and then averaging over all measurements. In other words, instead of M measurement devices, we employ ML to improve the performance. We call L the *hardware budget factor* as it indicates the number of measurement devices that we employ.

In this case, the probability of false alarm will be still expressed as in (13) while the lower and upper bounds for probability of detection are modified as

$$P_{D,lb} = \mathbb{Q}_{F(M_1N_b,M_2N_b)}\left(\frac{\sigma_0^2 + L\sigma_x^2\rho_{N-M_2+1}^2 + M\delta^{-1}}{\sigma_0^2 + L\sigma_x^2\rho_{M_1}^2 + M\delta^{-1}}\gamma\right), \tag{55}$$

and

$$P_{D,ub} = \mathbb{Q}_{F(M_1N_b,M_2N_b)}\left(\frac{\sigma_0^2 + L\sigma_x^2\rho_{N}^2 + M\delta^{-1}}{\sigma_0^2 + L\sigma_x^2\rho_{1}^2 + M\delta^{-1}}\gamma\right), \tag{56}$$

Comparing (55) and (56) with (15) and (16), the hardware budget factor L for achieving a performance similar or better than the infinite precision case of $\delta^{-1} = 0$ is obtained as

$$L \geq 1 + \frac{M}{\delta\sigma_0^2}. \tag{57}$$

B. Compressive Detection Using a Fixed Set of Measurement Vectors

The second model in this section for modeling non-ideal measurement devices is formulated as choosing the measurement vectors from a fixed set of unit-norm orthogonal vectors whose members are not necessarily singular vectors of the system matrix $\mathbf{H}$. These vectors can be hardware-realizable approximation of the singular vectors, e.g. quantized versions of them, or simple down-samplers. Assume that $M = M_1 + M_2$ measurement vectors should be chosen out of $R \geq M$ uncorrelated columns of $N \times R$ matrix $\mathbf{\Psi} = [\boldsymbol{\psi}_1, \boldsymbol{\psi}_2, \ldots, \boldsymbol{\psi}_R]$ (notice that $M\mathbf{\Psi}^T\mathbf{\Psi} = \mathbf{I}_R$). The rows of $\mathbf{\Phi}_s$ and $\mathbf{\Phi}_o$ then have to be chosen from the columns of $\mathbf{\Psi}$.

The optimum $\mathbf{\Phi}_s$ is the one that maximizes the energy of its output. If we want to follow the Maximally-Uncorrelated design of Section III-A, then the rows of $\mathbf{\Phi}_s$ are the M_1 columns of $\mathbf{\Psi}$ for which $\|\mathbf{\Phi}_s\mathbf{H}\|_F$ is maximized, i.e.,

$$\mathbf{\Phi}_s = \underset{\mathbf{\Psi}_{\mathcal{M}}^T}{\arg} \max_{\mathcal{M}\subset\mathcal{R}:|\mathcal{M}|=M_1} \mathrm{trace}(\mathbf{H}\mathbf{H}^T\mathbf{\Psi}_{\mathcal{M}}\mathbf{\Psi}_{\mathcal{M}}^T), \tag{58}$$

where $\mathcal{R} = \{1, 2, \ldots, R\}$ and $\mathbf{\Psi}_{\mathcal{M}}$ is the sub-matrix of $\mathbf{\Psi}$ consisting of columns determined by index set $\mathcal{M}$. Similarly, the rows of $\mathbf{\Phi}_o$ can be selected as the M_2 columns of $\mathbf{\Psi}$ for which $\|\mathbf{\Phi}_s\mathbf{H}\|_F$ is minimized,

i.e.,

$$\mathbf{\Phi}_o = \underset{\mathbf{\Psi}_{\mathcal{M}}^T}{\arg} \min_{\mathcal{M}\subset\mathcal{R}:|\mathcal{M}|=M_2} \mathrm{trace}(\mathbf{H}\mathbf{H}^T\mathbf{\Psi}_{\mathcal{M}}\mathbf{\Psi}_{\mathcal{M}}^T) \tag{59}$$

On the other hand, If we want to follow the Fully-Correlated design of Section III-B, then we should pick the two columns of $\mathbf{\Psi}$, say $\boldsymbol{\psi}_i$ and $\boldsymbol{\psi}_j$, that, respectively, maximize and minimize the signal energy $\sigma_x^2\boldsymbol{\psi}^T\mathbf{H}\mathbf{H}^T\boldsymbol{\psi}$ and then design $\mathbf{\Phi}_s$ and $\mathbf{\Phi}_o$, respectively, as

$$\mathbf{\Phi}_s \triangleq \frac{1}{\sqrt{M}}\mathbf{1}_{M_1,1}\otimes\boldsymbol{\psi}_i^T, \tag{60}$$

and

$$\mathbf{\Phi}_o \triangleq \frac{1}{\sqrt{M}}\mathbf{1}_{M_2,1}\otimes\boldsymbol{\psi}_j^T. \tag{61}$$

To see the performance of the detectors in this case, we first provide the detector's formulation when the noise variance is known. It is easy to verify that when the elements of $\mathcal{M}$ are orthonormal, P_{FA} is computed as in (44) and (49) for the Maximally-Uncorrelated and Fully-Correlated detectors, respectively. However, P_{D} of Fully-Correlated detector as well as the bounds of P_{D} of Maximally-Uncorrelated detector will differ from what we have in (46), (47) and (50). The reason for this is that the rows of $\mathbf{\Phi}_s$ are not any longer the singular vectors of $\mathbf{H}$ and therefore the set of singular values of $\mathbf{\Phi}_s\mathbf{H}$ is not a subset of the set of singular values of $\mathbf{H}$. In other words, (46), (47) and (50) should be respectively replaced by the following equations

$$P_{D,lb} = \mathbb{Q}_{\chi^2(M_1N_b)}(\tilde{\eta}_{lb}\gamma), \tag{62}$$

and

$$P_{D,ub} = \mathbb{Q}_{\chi^2(M_1N_b)}(\tilde{\eta}_{ub}\gamma), \tag{63}$$

and

$$P_{\text{D}} = \mathbb{Q}_{\chi^2(N_b)}\Big(\frac{\sigma_0^2}{\sigma_0^2+M_1\sigma_x^2\tilde{\rho}_1^2}\gamma\Big). \tag{64}$$

where $\tilde{\eta}_{lb} \triangleq \frac{\sigma_0^2}{\sigma_0^2+\sigma_x^2\tilde{\rho}_{M_1}^2}$, $\tilde{\eta}_{ub} \triangleq \frac{\sigma_0^2}{\sigma_0^2+\sigma_x^2\tilde{\rho}_1^2}$, and $\tilde{\rho}_1$ and $\tilde{\rho}_{M_1}$ are the greatest and smallest singular values of $\mathbf{\Phi}_s\mathbf{H}$, respectively. Since the eigenvalues of $\mathbf{H}\mathbf{H}^T\mathbf{\Phi}_s^T\mathbf{\Phi}_s$ are smaller than the corresponding eigenvalues of $\mathbf{H}\mathbf{H}^T$ [19, Theorem 6.76], the performance is lower than those indicated in (46), (47) and (50).

When the variance of noise is unknown, on the other hand, we cannot write the probability of detection of the detector based on F-distribution as the outputs of $\mathbf{\Phi}_s$ and $\mathbf{\Phi}_o$ measurement devices are not independent of each other, which is in turn because the rows of $\mathbf{\Phi}_s$ and $\mathbf{\Phi}_o$ are not any longer the singular

vectors of $\mathbf{H}$. However, we can still design a constant false alarm rate detector since in the absence of signal term $\mathbf{Hx}$ the output of these two measurement devices are still independent as $\mathbf{\Phi}_s^T\mathbf{\Phi}_o = \mathbf{0}$.

V. Compressive Detection on a Finite Union of Subspaces

In this section, we generalize the results of previous sections to the case when we know that the $\mathbf{H} \in \mathcal{S}$ where

$$\mathcal{S} = \{\mathbf{H}_1, \mathbf{H}_2, \ldots, \mathbf{H}_Q\}, \tag{65}$$

where $\mathbf{H}_q,\ q = 1, \ldots, Q$, is a full-column rank $N \times K_i$ matrix and the probability that the signal lies in subspace $\mathbf{H}_q$ is $\mathbb{P}(\mathbf{H} = \mathbf{H}_q) = \pi_q,\ q = 1, \ldots, Q$. The goal is then to accomplish the test of (3).

Similar to the case of $Q = 1$, the measurement matrix is tailored to performing the F-test. In other words, it must consist of two parts: one lying in the strongest signal subspace, which attains the maximum energy, and the other in the weakest subspace, which attains the minimum energy. But, since the true q is not known a priori, we should design it such that the expected value of the energy over the set $\mathcal{S}$ gets its maximum value for the first part and its minimum value for the second part.

To be more precise, if we design the subspace compressive detector based on Maximally-Uncorrelated strategy, the first and the second sets of measurement devices will be chosen as

$$\mathbf{\Phi}_s = \arg\max_{\mathbf{\Phi}} \mathbb{E}_{\mathbf{H},\mathbf{x},\mathbf{w}}(\mathbf{z}^T\mathbf{z}),\ \text{s.t. } M\mathbf{\Phi}\mathbf{\Phi}^T = \mathbf{I}_{M_1}. \tag{66}$$

and

$$\mathbf{\Phi}_o = \arg\min_{\mathbf{\Phi}} \mathbb{E}_{\mathbf{H},\mathbf{x},\mathbf{w}}(\mathbf{z}^T\mathbf{z}),\ \text{s.t. } M\mathbf{\Phi}\mathbf{\Phi}^T = \mathbf{I}_{M_2}, \tag{67}$$

respectively. On the other hand if we want to design it based on Fully-Correlated strategy we have to relax the constraints $M\mathbf{\Phi}\mathbf{\Phi}^T = \mathbf{I}$ in (66) and (67). This will guarantee that the energy of the signals collected at the first and second channels attain, respectively, the maximum and minimum possible values which can then be exploited for optimum compressive signal detection.

Theorem 5. *The first and second channels of measurement matrix which satisfy (66) and (67) are respectively the strongest signal eigenvectors and null eigenvectors of the following matrix*

$$\mathbf{H}_{\text{eq}} = \sum_{q=1}^{Q} \pi_q \mathbf{H}_q \mathbf{H}_q^T, \tag{68}$$

Proof: It is easy to see that

$$\begin{aligned}\mathbb{E}_{\mathbf{H},\mathbf{x},\mathbf{w}}(\mathbf{z}^T\mathbf{z}) &= \mathbb{E}_{\mathbf{H}}\Big(\sigma_x^2\mathrm{trace}(\mathbf{H}\mathbf{H}^T\mathbf{\Phi}^T\mathbf{\Phi}) + \frac{\sigma_0^2}{M}\Big) \\ &= \sum_{q=1}^{Q}\pi_q\sigma_x^2\mathrm{trace}(\mathbf{H}_q\mathbf{H}_q^T\mathbf{\Phi}^T\mathbf{\Phi}) + \frac{\sigma_0^2}{M}. \\ &= \sigma_x^2\mathrm{trace}(\mathbf{H}_{\mathrm{eq}}\mathbf{\Phi}^T\mathbf{\Phi}) + \frac{\sigma_0^2}{M}.\end{aligned} \tag{69}$$

Since the second term in the right-hand side of (69) is independent of the choice of measurement matrix, the measurements corresponding to the maximum and minimum variance are those which maximize and minimize the first term, which are the strongest M_1 eigenvectors and weakest M_2 eigenvectors, respectively. ■

Remark 1: The ordinary compressive detection can be specified as a particular case of the setting in this section. To see this, assume that we have a K-sparse signal in N-dimensional basis $\mathbf{\Psi}$ as

$$\mathbf{y} = \mathbf{\Psi}\mathbf{x}, \tag{70}$$

where $\mathbf{y}$ and $\mathbf{x}$ are both vectors of size N and only $K \ll N$ entries of $\mathbf{x}$ are nonzero. In the absence of any further structure, any K entries of $\mathbf{x}$ can be its true support set equally likely with probability $1/\binom{N}{K}$. In this case, each element of the union set $\mathcal{S}$ in (65) will be a size-K combination of the N columns of $\mathbf{\Psi}$. Furthermore, we will have $Q = \binom{N}{K}$ and $\pi_1 = \ldots = \pi_Q = \frac{1}{Q}$.

If the basis $\mathbf{\Psi}$ is orthonormal, then it is easy from (68) to verify that

$$\mathbf{H}_{\mathrm{eq}} = \frac{K}{N}\mathbf{I}_N. \tag{71}$$

Since all the singular values of $\mathbf{H}_{\mathrm{eq}}$ in (71) are equal, then $\mathbf{H}_{\mathrm{eq}}$ has no *structure* and therefore the methods proposed in Sections III-A and III-B are not suitable for detection of this signal[1] but we can use the method of Section III-C provided that the noise variance is known. However, if there is a known structure in the sparse random signal model of (70), for instance if the probability of different K-size combinations are not equal or if $\mathbf{\Psi}$ is not an orthonormal basis, in the sense that not all of the singular values of $\mathbf{H}_{\mathrm{eq}}$ are identical, then the methods proposed in Sections III-A and III-B can be employed for detection of signal from compressive measurements.

[1]Notice that in the absence of noise variance knowledge, none of the methods in the literature can detect the signal.

VI. Simulation Results

In this section we study the performance of the proposed compressive detection methods via some simulation studies.

The first experiment is to compare the performance of the two methods proposed in Sections III-A and III-B which are able to detect the signal under unknown variance condition. In this experiment we choose $N = 1000$ and $K = 10$. The elements of matrix $\mathbf{H}$ are generated independently from $\mathcal{N}(0, 1/\sqrt{K})$ such that the expected value of the squared second norm of its rows is one. Signal $\mathbf{x}$ and noise $\mathbf{w}$ are both drawn from zero-mean Gaussian distribution with variances σ_s^2 and σ_0^2, respectively. We define the SNR as $10\log_{10}\frac{\sigma_x^2}{\sigma_0^2}$ (in dB). The number of measurement devices is $M \in \{2, 4, 8\}$ and we choose $M_1 = M_2 = M/2$. The results are obtained from 10000 random trials to gather sufficient statistics for reliable evaluation of the performance.

Figure 2 illustrates the performance in terms of probability of detection as a function of $\frac{\sigma_x^2}{\sigma_0^2}$. The curves have been depicted for two cases of $N_b = 5$ and $N_b = 50$. As it can be observed, while Maximally-Uncorrelated compressive detector provides better performance for smaller N_b at high SNRs, it becomes inferior to Fully-Correlated detector for higher N_b's and at lower SNRs. This is also clear from Figure 3 where the performance in terms of Receiver Operating Characteristics (ROC) has been depicted. As we can see, again Maximally-Uncorrelated compressive detector outperforms Fully-Correlated method for high SNRs and small N_b's, while Fully-Correlated method works better in small SNRs and for higher number of measurement devices.

The second experiment is to study the performance loss caused by the lack of knowledge about the noise variance. Figures 4 and 5 show the performance of the proposed Maximally-Uncorrelated detection method for two cases: when the noise variance is known and when it is unknown. As we expect, the lack of knowledge of noise variance results in considerable performance degradation. However, reasonable performance is still obtained.

In the third experiment we study the effect of imprecise measurements and compensating it by deploying multiple measurement devices. The imprecision is modeled as described in Section IV-A. Figure 6 illustrates the ROC curves for precise (red curves) and imprecise (blue curves) measurements when $\sigma_s^2 = 1$, and $\sigma_0^2 = 100$. The precision of all imprecise devices (blue curves) is chosen as $\delta = 0.01$. As expected and is clear from the comparison of the red curve with blue curve with $L = 1$, in equivalent number of measurement devices, the imprecision in measurements results in a considerable loss in performance. However, this can be compensated by employing higher number of measurement devices.

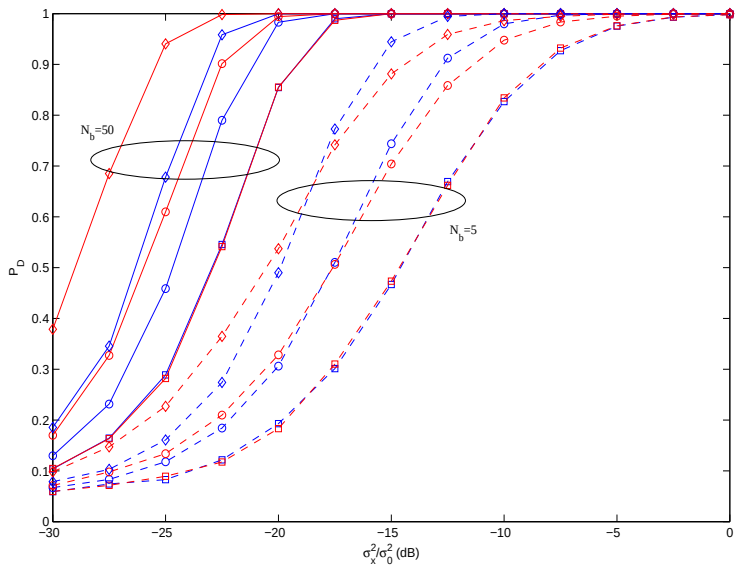

Fig. 2. Probability of Detection as a function of SNR for Maximally-Uncorrelated compressive detector (Blue) versus Fully-Correlated method (Red) when $P_{\text{FA}} = 0.05$. Solid curves represent the case when $N_b = 50$, and dashed curves represent the case when $N_b = 5$. The number of measurement devices is $M = 2$ (square), $M = 4$ (circle), and $M = 8$ (diamond). Furthermore we choose $M_1 = M_2 = M/2$.

For instance, when $L = 3$, the performance becomes equivalent to the precise case. This can be also verified by (57) in which the lower bound for performance improvement is $L = 3$. When we go beyond this bound, e.g. $L = 5$, the performance improves compared to the precise case.

Figure 7 shows how the probability of detection changes with the noise power for various precisions and hardware budgets of $L \in \{1, 3\}$. The black curve depicts the performance with a single precise device. Here the performance enhancement with deploying $L = 3$ times devices has been depicted. As it can be seen for a certain δ, the performance of the case of $L = 3$ is better than a single precise device as long as $\sigma_0^2 < \frac{M}{L-1}\delta^{-1}$. On the other hand, when the variance of noise is higher than this limit, even employing L times devices is not enough for compensating the imprecision.

In the fourth experiment we study the performance of the proposed compressive detection method when the signal comes from a union of some subspaces with certain probabilities. For this experiment, the ambient dimension is $N = 20$ and the signal dimension is $K = 3$. In each random trial we first generate an $N \times N$ matrix with entries from a normal distribution with mean zero and variance $1/K$. The elements of union set $\mathcal{S}$ in (65) are then Q different K-size combinations of columns of the generated matrix

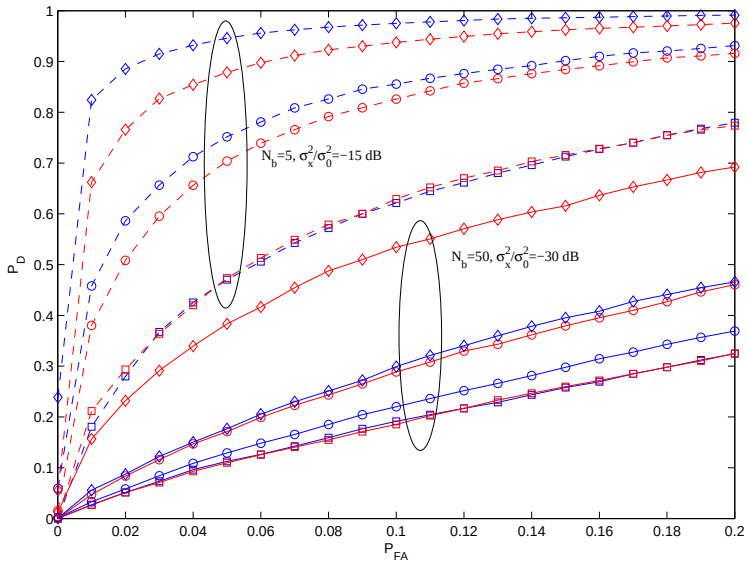

Fig. 3. ROC for Maximally-Uncorrelated compressive detector (Blue) versus Fully-Correlated method (Red). Solid curves represent the case when $N_b = 50$ and $\sigma_s^2/\sigma_0^2 = -30$ dB, and dashed curves represent the case when $N_b = 5$ and $\sigma_s^2/\sigma_0^2 = -15$ dB. The number of measurement devices is $M = 2$ (square), $M = 4$ (circle), and $M = 8$ (diamond). Furthermore we choose $M_1 = M_2 = M/2$.

while the signal is generated from one of them which is chosen uniformly randomly from all Q possible combinations. This implies that $\pi_1 = \ldots = \pi_Q = 1/Q$. The experiment is done for $Q \in \{1, 10, 50\}$. We remark that the case of $Q = 1$ coincides with the basic case described in Section III as in this case there is no uncertainty over the subspace on which signal lies.

Figure 8 illustrates the performance in terms of probability of detection for various values of σ_x^2/σ_0^2. The probability of false alarm here is set to $P_{\text{FA}} = 0.05$ and the number of measurements is $N_b = 50$. The results are shown for $M \in \{2, 4\}$ with $M_1 = M_2 = M/2$. Figure 9 also shows the ROC curves when $\sigma_x^2/\sigma_0^2 = -10dB$. As it can be seen, as the cardinality of the subspace union set $\mathcal{S}$ increases, the performance of the algorithm degrades. This is in turn because as the number of possible subspaces increases, the rows of measurement matrix $\mathbf{\Phi}$ are less matched to the singular vectors of the true subspace matrix.

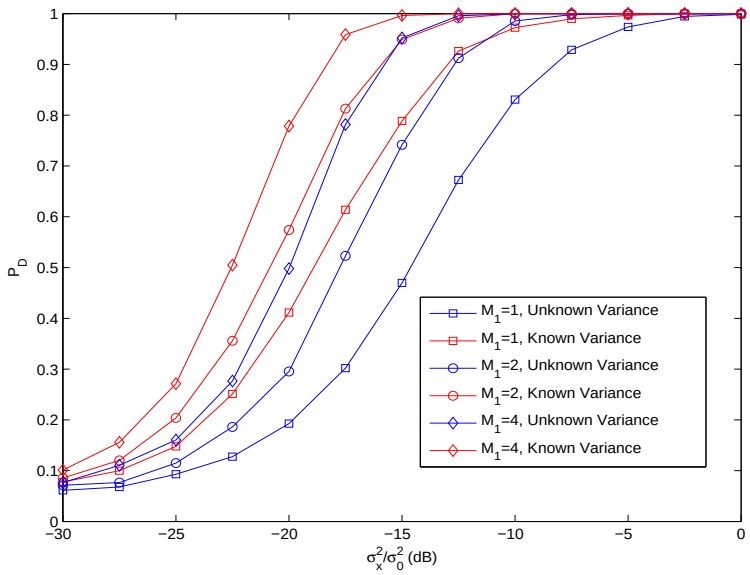

Fig. 4. Probability of Detection as a function of SNR of Maximally-Uncorrelated compressive detector for unknown variance (blue) versus known variance (red) when $P_{\text{FA}} = 0.05$. The number of measurements over time is $N_b = 5$. The number of rows of $\mathbf{\Phi}_s$ is $M_1 = 1$ (square), $M_1 = 2$ (circle), and $M_1 = 4$ (diamond). When the variance is known we have $M = M_1$ and when it is unknown we choose $M_2 = M_1$ and therefore we have $M = 2M_1$.

VII. Conclusion

The problem of signal detection from compressive measurements when the signal is lying (or leans toward) a low dimensional subspace was studied. Having the knowledge of the subspace signal, we proposed two measurement designs and formulated the hypothesis test and its performance metrics for each of them in the case that the noise variance is unknown. We also showed how the design can be simplified in the case that the noise variance is known. We analyzed the effects of imprecise measurements and showed how it can be compensated by deploying more identical measurement devices. The problem was also formulated for the case when signal belongs to a union of finite number of subspaces with known probabilities.

Acknowledgement

This work was supported by the Finnish Funding Agency for Technology and Innovation (Tekes) under the project ”Enabling Methods for Dynamic Spectrum Access and Cognitive Radio (ENCOR)”, and the

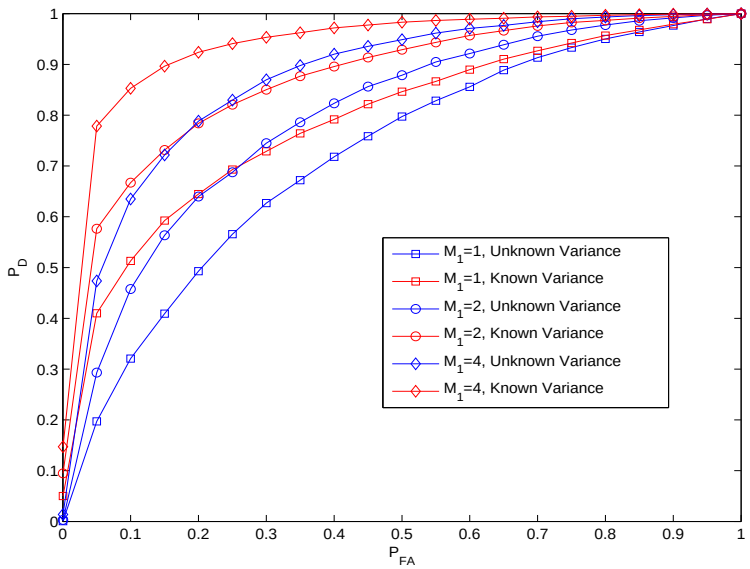

Fig. 5. ROC for Maximally-Uncorrelated detector for unknown variance (blue) versus known variance (red) when $N_b = 5$ and $\sigma_s^2/\sigma_0^2 = -20$ dB. The number of rows of $\mathbf{\Phi}_s$ is $M_1 = 1$ (square), $M_1 = 2$ (circle), and $M_1 = 4$ (diamond). When the variance is known we have $M = M_1$ and when it is unknown we choose $M_2 = M_1$ and therefore we have $M = 2M_1$.

Academy of Finland under the project $\#251138$ "Digitally-Enhanced RF for Cognitive Radio Devices (DECORA)".

REFERENCES

[1] D. Donoho, "Compressed sensing," *IEEE Transactions on Information Theory*, vol. 52, no. 4, pp. 1289 –1306, Apr. 2006.

[2] E. J. Candes and T. Tao, "Near-optimal signal recovery from random projections: Universal encoding strategies?" *IEEE Transactions on Information Theory*, vol. 52, no. 12, pp. 5406 –5425, dec. 2006.

[3] E. J. Candes and M. Wakin, "An introduction to compressive sampling," *Signal Processing Magazine, IEEE*, vol. 25, no. 2, pp. 21 –30, March 2008.

[4] M. A. Davenport, P. T. Boufounos, M. B. Wakin, and R. G. Baraniuk, "Signal processing with compressive measurements," *Selected Topics in Signal Processing, IEEE Journal of*, vol. 4, no. 2, pp. 445–460, 2010.

[5] M. A. Davenport, M. B. Wakin, and R. G. Baraniuk, "Detection and estimation with compressive measurements."

[6] J. Paredes, Z. Wang, G. R. Arce, and B. M. Sadler, "Compressive matched subspace detection," in *Proc. 17th European Signal Processing Conference (EUSIPCO)*. Citeseer, 2009, pp. 120–124.

[7] Z. Wang, G. R. Arce, and B. M. Sadler, "Subspace compressive detection for sparse signals," in *Acoustics, Speech and Signal Processing, 2008. ICASSP 2008. IEEE International Conference on*, 2008, pp. 3873–3876.

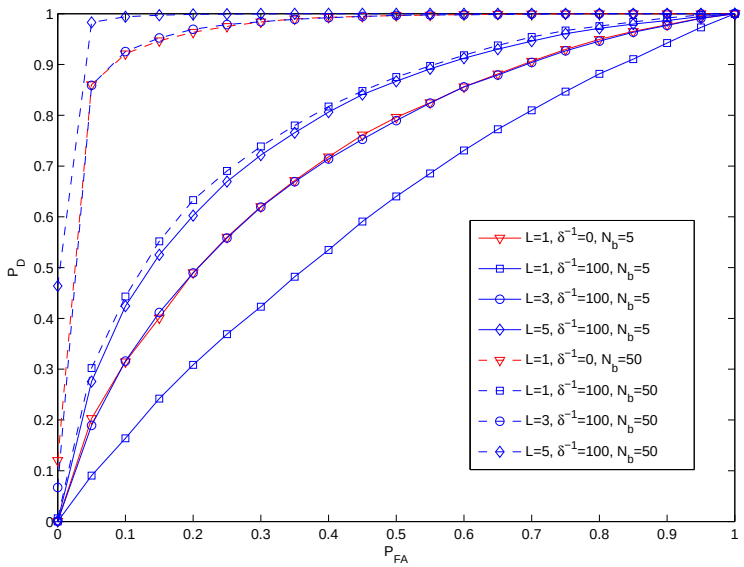

Fig. 6. ROC for imprecise measurements (blue curves) versus precise measurements (red curves). Solid curves represent the case when $N_b = 5$ and dashed curves represent the case when $N_b = 50$. We have chosen $\sigma_s^2 = 1$, and $\sigma_0^2 = 100$. The number of measurement devices in precise case is $M = 2$ with $M_1 = M_2 = 1$. For imprecise measurements, the device multiplicity has been chosen as $L \in \{1, 3, 5\}$.

[8] R. Zahedi, A. Pezeshki, and E. K. Chong, "Measurement design for detecting sparse signals," *Physical Communication*, vol. 5, no. 2, pp. 64–75, 2012.

[9] M. Azizyan and A. Singh, "Subspace detection of high-dimensional vectors using compressive sampling," in *Statistical Signal Processing Workshop (SSP), 2012 IEEE*. IEEE, 2012, pp. 724–727.

[10] B. S. M. R. Rao, S. Chatterjee, and B. Ottersten, "Detection of sparse random signals using compressive measurements," in *Acoustics, Speech and Signal Processing (ICASSP), 2012 IEEE International Conference on*. IEEE, 2012, pp. 3257–3260.

[11] J. Haupt, R. Castro, R. Nowak, G. Fudge, and A. Yeh, "Compressive sampling for signal classification," in *Signals, Systems and Computers, 2006. ACSSC'06. Fortieth Asilomar Conference on*. IEEE, 2006, pp. 1430–1434.

[12] M. F. Duarte, M. A. Davenport, M. B. Wakin, J. N. Laska, D. Takhar, K. F. Kelly, and R. G. Baraniuk, "Multiscale random projections for compressive classification," in *Image Processing, 2007. ICIP 2007. IEEE International Conference on*, vol. 6. IEEE, 2007, pp. VI–161.

[13] H. Reboredo, F. Renna, R. Calderbank, and M. R. Rodrigues, "Compressive classification," in *Information Theory Proceedings (ISIT), 2013 IEEE International Symposium on*. IEEE, 2013, pp. 674–678.

[14] M. A. Davenport, M. F. Duarte, M. B. Wakin, J. N. Laska, D. Takhar, K. F. Kelly, and R. G. Baraniuk, "The smashed filter for compressive classification and target recognition," in *Electronic Imaging 2007*. International Society for Optics and Photonics, 2007, pp. 64 980H–64 980H.

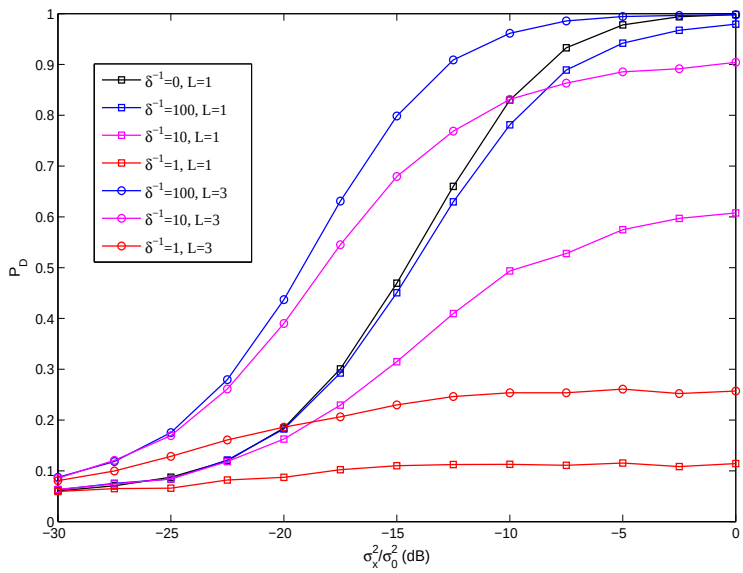

Fig. 7. Probability of detection for different precisions and device multiplicity values. The number of measurements per device is $N_b = 5$. We have chosen $\sigma_s^2 = 1$.

[15] S. Kay, *Fundamentals of statistical signal processing: detection theory*. Prentice Hall, 1998.

[16] H. V. Poor, *An introduction to signal detection and estimation*. Springer Science & Business Media, 1994.

[17] L. L. Scharf, *Statistical Signal Processing: Detection, Estimation, and Time Series Analysis*. Addison Wesley Publishing Company, 1991.

[18] C. R. Rao and M. B. Rao, *Matrix algebra and its applications to statistics and econometrics*. World Scientific, 1998.

[19] G. A. F. Seber, *A Matrix Handbook for Statisticians*. Wiley-Interscience, 2008.

[20] F. Zhang, *Matrix theory: basic results and techniques*. Springer Science & Business Media, 2011.

[21] N. L. Johnson, S. Kotz, and N. Balakrishnan, "Continuous univariate distributions, vol. 2 of wiley series in probability and mathematical statistics: applied probability and statistics," 1995.

[22] A. W. Marshall, I. Olkin, and B. C. Arnold, *Inequalities: Theory of majorization and its applications: Theory of majorization and its applications*. Springer Science & Business Media, 2010.

[23] L. L. Scharf and B. Friedlander, "Matched subspace detectors," *Signal Processing, IEEE Transactions on*, vol. 42, no. 8, pp. 2146–2157, 1994.

[24] J. Haupt, R. M. Castro, and R. Nowak, "Distilled sensing: Adaptive sampling for sparse detection and estimation," *Information Theory, IEEE Transactions on*, vol. 57, no. 9, pp. 6222–6235, 2011.

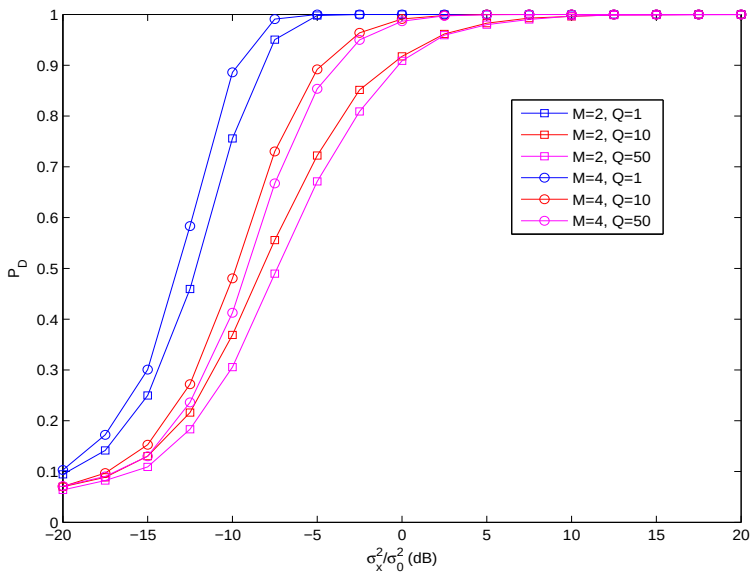

Fig. 8. Probability of Detection versus σ_x^2/σ_0^2 (in dB) for various numbers of measurement devices and cardinalities of the union set. The number of measurements in time is $N_b = 50$.

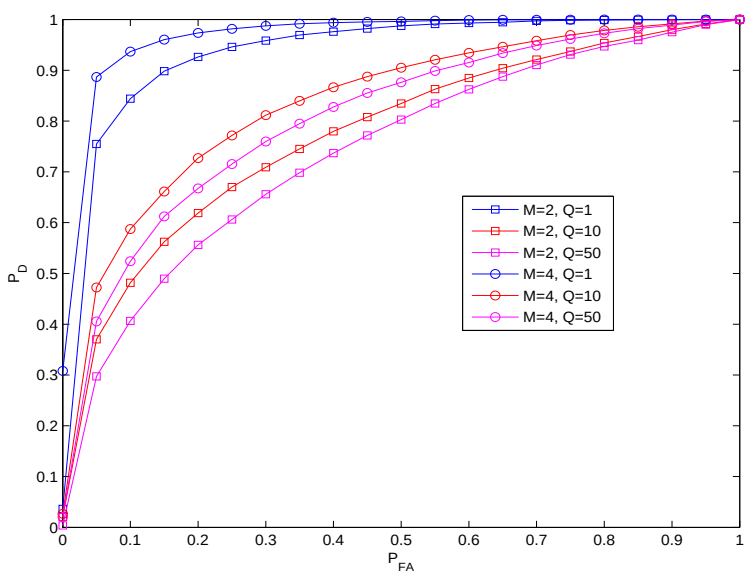

Fig. 9. ROC curves for various numbers of measurement devices and cardinalities of the union set. The number of measurements is $N_b = 50$ and the SNR is $\sigma_x^2/\sigma_0^2 = -10$ dB.